A novel composite UV/blue photodetector based on CMOS technology: design and simulation*

CHEN Chang-ping (陈长平)[1], **JIN Xiang-liang** (金湘亮)[1]**, **and LUO Jun** (罗均)[2]
1. Faculty of Materials, Optoelectronics and Physics, Xiangtan University, Xiangtan 411105, China
2. Faculty of Precision Mechanical Engineering, Shanghai University, Shanghai 200444, China

(Received 27 August 2013)

A novel composite ultraviolet (UV)/blue photodetector is proposed in this paper. Lateral ring-shaped PN junction is used to separate photogenerated carriers and inject the non-equilibrium excess carriers to the bulk, changing the bulk potential and shifting the threshold voltage of the metal-oxide-semiconductor field-effect transistor (MOSFET) as well as the drain current. Numerical simulation is carried out, and the simulation results show that the composite photodetector has the enhanced responsivity for UV/blue spectrum. It exhibits very high sensitivity to weak and especially ultra-weak light. A responsivity of 7000 A/W is obtained when the photodetector is illuminated under incident optical power of 0.01 μW. As a result, this proposed combined photodetector has great potential for UV/blue and ultra-weak light applications.
Document code: A **Article ID:** 1673-1905(2013)06-0414-4
DOI 10.1007/s11801-013-3149-5

Ultraviolet (UV) detection technology is developed after the infrared and laser detection technology. UV detectors are researched and used in many application areas, such as environmental monitoring[1] and biochemical analysis[2]. Photodiodes used for UV detecting are required to be sensitive to blue/UV radiation and blind to visible and near-infrared radiation. Different structures of silicon-based UV/blue photodiodes have been reported in Refs.[3-5]. The first UV avalanche photodiode in complementary metal-oxide-semiconductor (CMOS) technology[5] achieved a responsivity of 2.3 A/W at 400 nm for a reverse bias of 19.1 V. Recently, the development of phototransistors for UV/blue detection has attracted much interest[6-8]. However, all of the researches haven't solved the problem of low UV/blue responsivity. Numerical methods are adopted to analyze the characteristics of floating-body transistors, photo-gate transistors and quadruple gate transistors[9-11].

In this paper, a new combined photodetector with enhanced sensitivity to UV/blue and ultra-weak light is proposed, and its operating principle is presented. Numerical simulation is adopted to analyze its photoelectric characteristics. The variations of threshold voltage, output, optical response and direct current (DC) characteristics before and after illumination are simulated and analyzed, respectively.

The device structure of the combined photodetector is shown in Fig.1, which consists of an N-channel MOS (NMOS) transistor and a lateral photodiode. For the NMOS, the N^+ source is placed in the center with ring-shaped poly-silicon gate and N^+ drain. For the photodiode, the P_{well} (B, bulk) is enclosed by the ring-shaped N_{well} (C, cathode), and they form the lateral PN junction.

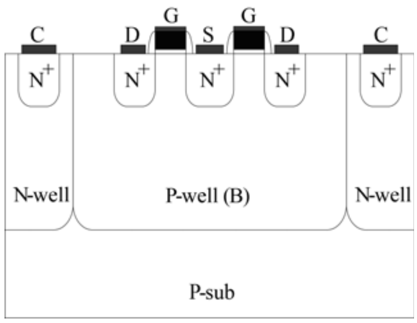

Fig.1 Structure of the combined photodetector with NMOS transistor

The P_{well} bulk is set floating and the lateral P_{well}/N_{well} junction is used to separate photogenerated electron-hole pairs[12,13]. The photogenerated carriers drifting into the bulk can change the P_{well} bulk potential, and further change the threshold voltage as well as the output drain current. The main purpose to design a ring-shaped structure is to enhance its sensitivity to UV/blue spectrum, because most photogenerated carriers are very close to the surface (within 150 nm) for the UV/blue incident

* This work has been supported by the National Natural Science Foundation of China (Nos.61233010 and 61274043), and the Program for New Century Excellent Talents in University of Ministry of Education of China (No.NCET-11-0975).
** E-mail: jinxl@xtu.edu.cn

light. The depletion region of the lateral P_{well}/N_{well} photodiode near the silicon surface is enlarged by using the proposed ring-shaped layout. Much more photogenerated carriers drift into the P_{well} bulk and cause a larger shift of the threshold voltage, which determine a larger photocurrent.

The P_{well}-N_{well} voltage V_{BC}, resulting from the illumination, can be described by the transposed diode equation[14] as

$$V_{BC} = V_T \cdot \ln\left(1 + \frac{I_{BC}}{I_0}\right) = V_T \cdot \ln\left(1 + \frac{F \cdot P_{opt}}{I_0}\right), \quad (1)$$

where V_T is the thermal voltage, I_{BC} is the photocurrent of the lateral photodiode, P_{opt} is the incident light power, and F is a function of material parameters, transistor bias voltages and depletion region area of the P_{well}/N_{well} junctions. The P_{well}-source voltage V_{BS} is equal to the sum of the P_{well}-N_{well} voltage V_{BC} and the N_{well}-source voltage V_{CS} as

$$V_{BS} = V_{BC} + V_{CS} . \quad (2)$$

Considering the carriers injected from N_{well} into P_{well}, the threshold voltage after illumination can be defined as

$$V_{TH} = \phi_{ms} - \frac{Q_{ox}}{C_{ox}} + \frac{\sqrt{2\varepsilon_{Si} q N_D (2\phi_f - V_{BS})}}{C_{ox}} + 2V_T \cdot \frac{N_D}{n_i}, \quad (3)$$

where ϕ_{ms}, Q_{ox}, C_{ox}, ε_{Si}, q, N_D, n_i and ϕ_f are the metal-semiconductor work function difference, the fixed charge in the gate oxide layer, the gate oxide capacitance, the permittivity of silicon, the unit electric charge, the density of donor impurity, the intrinsic concentration of electron and the fermi potential, respectively.

It is supposed that the majority carriers can be exhausted in the depletion region x_d on the silicon surface of the MOS capacitance. By analyzing the modeled structure in Fig.2, the total signal charges $Q_s(y)$ can be given as[10]

$$Q_s(y) = C_{ox}\left\{-\left[\left(V_G - V_{FB}\right) - 2\psi_F + \frac{V_0}{2} - V(y)\right] + \sqrt{\left(V_G - V_{FB}\right) + 2\psi_F + \frac{V_0}{4} + V(y)}\right\}, \quad (4)$$

where $V_0 = qN_A\varepsilon_{Si}/C_{ox}^2$. V_{FB}, N_A, ψ_F and $V(y)$ are the flat band voltage, the density of acceptor impurity, the fermi level during the P-substrate and the potential drop along the y-orientation at the beginning of the strong inversion, respectively.

Two concepts used in the current-voltage derivation are charge neutrality and Gauss's law[15]. The inversion layer charge per unit area is shown as

$$Q_n = C_{ox}\left[\left(V_{GS} - V_y\right) - V_{TH}\right] + Q_s(y), \quad (5)$$

where V_{GS} is the gate-source voltage and V_y is the potential in the channel at a point y along the channel length.

The total channel current is given as

$$I_y = -W\mu_n\left\{C_{ox}\left[\left(V_{GS} - V_y\right) - V_{TH}\right] + Q_s(y)\right\}\frac{dV_y}{dy}, \quad (6)$$

where W is the channel width, and μ_n is the electron mobility.

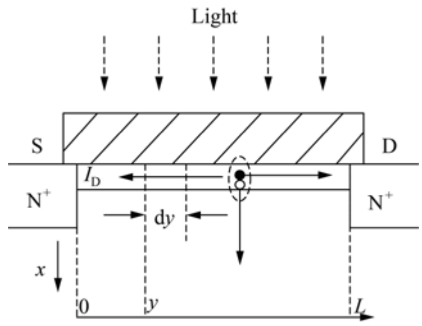

Fig.2 Schematic diagram of analytical model for current-voltage characteristics of the NMOS transistor

Assuming μ_n is constant and letting $I_D = -I_y$ since drain current is constant along the entire channel, the drain current I_D can be obtained by integrating Eq.(6). The drain current can be induced by

$$\int_0^L I_D dy = \int_0^L W\mu_n\left\{C_{ox}\left[\left(V_{GS} - V_y\right) - V_{TH}\right] + Q_s(y)\right\}dV_y . \quad (7)$$

The photocurrent response I_{ph} is the difference of two output drain current values, and refers to the DC responsivity of the device defined as the absolute of output current difference divided by the incident optical power, which can be expressed as

$$R_{dc} = \left|I_D - I_{D0}\right|/P, \quad (8)$$

where I_{D0} is the drain current without illumination as

$$I_{D0} = \frac{W\mu_n C_{ox}}{2L}\cdot\left[2(V_{GS} - V_{TH0})V_{DS} - V_{DS}^2\right]. \quad (9)$$

Simulation under a certain bias voltage condition (V_{source}=0 V, V_{drain}=0.1 V and $V_{cathode}$=3 V) is conducted to testify the threshold voltage variation. Different incident optical power values are chosen, and the gate voltage is swept from 0 V to 3 V. As shown in Fig.3, the threshold voltage decreases after illumination, and the stronger the incident optical power is, the smaller the threshold voltage of the NMOS transistor is.

Drain current values of the NMOS transistor with and without illumination are simulated and analyzed. The source is grounded, and the cathode is fixed at a bias voltage of 3 V. Sweep the drain voltage from 0 V to 3 V when the gate voltage is stepped from 0 V to 3 V. As shown in Fig.4, both of the drain current values with and without illumination are zero if the gate voltage is fixed at 0 V. The drain current increases significantly when the gate voltage reaches the threshold voltage of the NMOS transistor. And the difference of the two drain current values with and without illumination becomes bigger when the gate voltage is larger. In other words, the drain current affected by light illumination is more obvious.

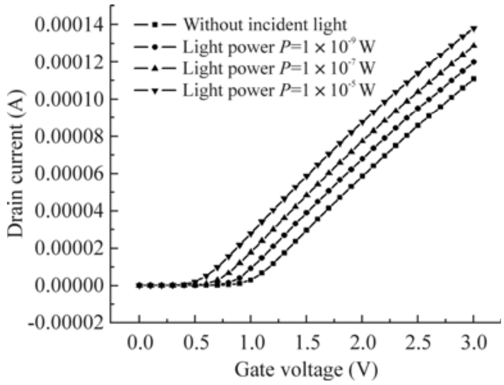

Fig.3 Drain current vs. gate voltage with different light intensity illuminations

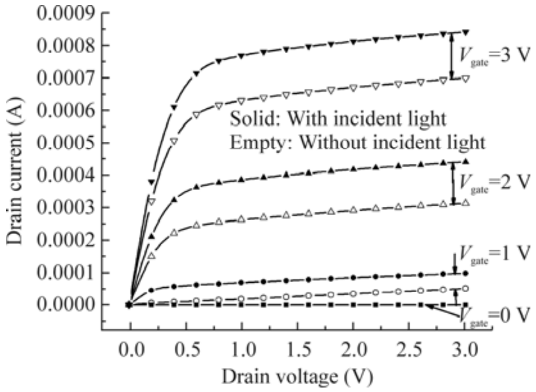

Fig.4 Drain current of the NMOS transistor with and without illumination

Spectral response characteristics of the proposed combined photodetector are studied to verify that it has an enhanced responsivity for UV/blue light. The source is grounded, and the gate, the drain and the cathode are applied with a voltage of 3 V at the same time. Simulation results are shown in Fig.5. The drain current of the NMOS transistor is almost constant for the light with wavelength less than 600 nm. The drain current begins to decrease when the wavelengh is longer than 600 nm. So its UV/blue responsivity is better than its visible and infrared responsivity (with wavelength longer than 700 nm). This new combined photodetector shows the enhanced UV responsivity compared with conventional silicon UV photodiodes.

The DC response curves are shown in Fig.6. The DC response is very small if gate voltage of the device is zero, and it increases significantly when the gate voltage is fixed at a certain bias, such as 1 V. The values of the DC response are almost the same when the gate biases are 2 V and 3 V, respectively. From another point of view, it shows that the larger the incident optical power is, the smaller the DC response is. The DC responsivity increases rapidly if the incident optical power is smaller than a certain value. For example, when the gate voltage is 3 V and the incident power is 0.01 μW, the device obtains a DC responsivity of 7000 A/W. It increases the responsivity by 35000 times compared with traditional silicon-based UV photodiodes whose responsivity is only about 0.2 A/W. Therefore, the proposed combined photodetector in this paper has high potential application in UV and ultra-weak light detections.

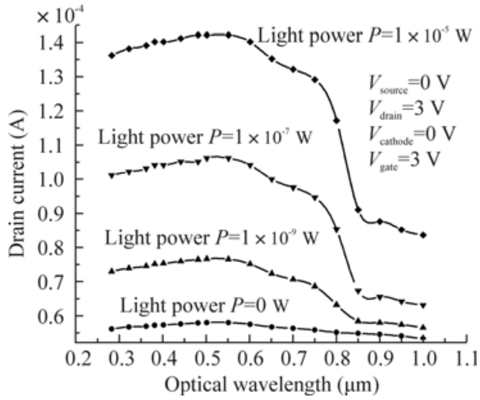

Fig.5 Drain current vs. wavelength with different incident light power

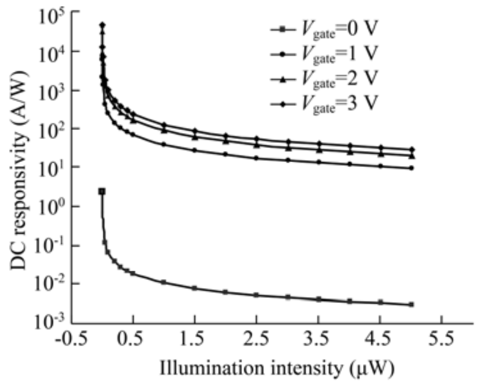

Fig.6 DC responsivity of the proposed combined photodetector

A new combined photodetector with enhanced sensitivity to UV/blue and ultra-weak spectrum is proposed. Numerical simulation is used to analyze its photoelectric characteristics. This new combined photodetector shows the enhanced UV responsivity compared with conventional silicon-based UV photodiodes. It increases the responsivity by five orders of magnitude compared with the traditional silicon-based UV photodiodes whose responsivity is about 0.2 A/W. And the spectral response characteristic for UV/blue light is better than that for visible/infrared light. Furthermore, the proposed combined photodetector has high potential application in ultra-weak light detections.

References

[1] Edoardo Charbon, J. Phys. D: Appl. Phys. **41**, 1 (2008).

[2] Y. W. Chang, P. C. Yu, Y. T. Huang and Y. S. Yang, A CMOS-Compatible Optical Biosensing System based on Visible Absorption Spectroscopy, IEEE Int. Conf. Electron Devices and Solid-State Circuits, 1099 (2007).

[3] A. Pauchard, P. A. Besse and R. S. Popovic, Sens. Actuators **76**, 172 (1999).

[4] A. Ghazi, H. A. Zimmermann and P. Seegebrecht, IEEE Trans. Electron Devices **49**, 1124 (2002).

[5] A. Pauchard, A. Rochas, Z. Randjelovic, P. A. Besse and R. S. Popovic, Ultraviolet Avalanche Photodiode in CMOS Technology, International Electron Decices Meeting Technical Digest, 709 (2000).

[6] Li Guike, Feng Peng and Wu Nanjian, Journal of Semiconductors **32**, 105008-1 (2011).

[7] SHAO Hui-min, ZHANG Shi-lin, XIE Sheng, LI Xian-jie, YIN Shun-zheng, CAI Dao-min and MAO Lu-hong, Journal of Optoelectronics·Laser **22**, 984 (2011). (in Chinese)

[8] Esmaeili-Rad M. R., Papadopoulos N. P., Bauza M., Nathan A. and Wong W. S., Electron Device Letters **33**, 567 (2012).

[9] Xiang-liang Jin, Jie C. and Yu-lin Qiu, Semiconductor Photonics and Technology **9**, 75 (2003).

[10] Wu W. J., Yao R. H., Chen T., Chen R. S. and Deng W. L., Solid-State Electronics **52**, 930 (2008).

[11] Gaffar M., Alam M., Ashraf Mamun S. and Matin A., Microelectronics Journal **42**, 808 (2011).

[12] Schanz M., Brockherde W., Hauschild R., Hosticka B. J. and Teuner A., CMOS Photosensor Arrays with on-chip Signal Processing, 23rd European Solid-State Circuits Conference, 236 (1997).

[13] LI Chang-sheng, YAO Jian, ZHANG Chun-xi and WANG Bo, Journal of Optoelectronics·Laser **23**, 1086 (2012). (in Chinese)

[14] S. M. Sze and K. K. Ng. Physics of Semiconductor Devices, 3rd ed. Hoboken, NJ: Wiley, 2007.

[15] Donald A. Neaman, Semiconductor Physics and Devices: Basic Principles (Photocopy Edition), 3rd ed., Beijing: Tsinghua University Press, 2003.